Analysis of transient fission gas behaviour in oxide fuel using BISON and TRANSURANUS

T. Barani[a], E. Bruschi[a], D. Pizzocri[a], G. Pastore[b], P. Van Uffelen[c], R.L. Williamson[b], L. Luzzi[a,*]

[a] *Politecnico di Milano, Department of Energy, Nuclear Engineering Division, via La Masa 34, I-20156 Milano, Italy*
[b] *Fuel Modeling and Simulation Department, Idaho National Laboratory, P.O. Box 1625, Idaho Falls, ID 83415-3840, United States*
[c] *European Commission, Joint Research Centre, Directorate for Nuclear Safety and Security, P.O. Box 2340, 76125 Karlsruhe, Germany*

Abstract

The modelling of fission gas behaviour is a crucial aspect of nuclear fuel performance analysis in view of the related effects on the thermo-mechanical performance of the fuel rod, which can be particularly significant during transients. In particular, experimental observations indicate that substantial fission gas release (FGR) can occur on a small time scale during transients (burst release). To accurately reproduce the rapid kinetics of the burst release process in fuel performance calculations, a model that accounts for non-diffusional mechanisms such as fuel micro-cracking is needed. In this work, we present and assess a model for transient fission gas behaviour in oxide fuel, which is applied as an extension of conventional diffusion-based models to introduce the burst release effect. The concept and governing equations of the model are presented, and the effect of the newly introduced parameters is evaluated through an analytic sensitivity analysis. The model is assessed for application to integral fuel rod analysis by implementation in two structurally different fuel performance codes: BISON (multi-dimensional finite element code) and TRANSURANUS (1.5D code). Model assessment is based on the analysis of 19 light water reactor fuel rod irradiation experiments from the OECD/NEA IFPE (International Fuel Performance Experiments) database, all of which are simulated with both codes. The results point out an improvement in both the quantitative predictions of integral fuel rod FGR and the qualitative representation of the FGR kinetics with the transient model relative to the canonical, purely diffusion-based models of the codes. The overall quantitative improvement of the integral FGR predictions in the two codes is comparable. Moreover, calculated radial profiles of xenon concentration after irradiation are investigated and compared to experimental data, illustrating the underlying representation of the physical mechanisms of burst release.

Keywords: fission gas, burst release, fuel modelling, BISON code, TRANSURANUS code

1. Introduction

Fission gas behaviour (FGB) modelling is an essential part of the thermo-mechanical analysis of nuclear fuel rods with fuel performance codes [1,2]. Due their low solubility, fission gases tend to be released to the rod free volume, increasing the rod inner pressure, or precipitate in the form of bubbles, causing fuel swelling thus promoting pellet-cladding mechanical interaction. Such processes affect the mechanical behaviour of the fuel rod. Moreover, fission gas release (FGR) can lower the thermal conductance of the fuel-cladding gap and gas precipitation into bubbles degrades the fuel thermal conductivity, both processes affecting the temperature distribution in the fuel pellets.

Modelling of FGB in oxide fuel under irradiation calls for the treatment of various interactive phenomena [1–5]. Diffusion to the grain boundaries of the gas generated within the fuel grains needs to be described along with intricate grain boundary processes. The latter involve precipitation and growth of lenticular bubbles at the grain faces contributing to fuel swelling, and eventual gas venting from the grain faces leading to thermal FGR. Venting occurs after extensive gas bubble growth and interconnection, driven by gas atom and vacancy diffusion to the bubbles [1,5]. In addition to this diffusion-based process, experimental observations suggest that gas release from the grain boundaries may occur through a mechanism of grain-face separation due to micro-cracking [6–10]. Such mechanism is thought to be responsible for the high FGR observed in transient tests, which is characterized by a rapid kinetics that cannot be explained as purely diffusion-controlled [6,8,11–16]. Such rapid FGR observed in transient tests is often referred to as 'burst release'.

Carroll et al. [6] ascribed an increase in the FGR rate observed during UO_2 irradiation experiments to micro-cracking along grain boundaries due to a combination of thermal stresses and stresses generated by the accumulation of fission gas. Rest and Gehl [7] experimentally observed planar separations on the grain surfaces in UO_2 fuel specimens after transient heating. They noted that cracking along a given grain-grain contact can only result in release of the gas stored at the grain surfaces. Examinations

*Corresponding author
Email address: Lelio.Luzzi@polimi.it (L. Luzzi)

of transient-tested UO_2 fuel rods performed by Hastings et al. [8] and by Walker et al. [9] also demonstrated the presence of grain-boundary separations. In both papers, microcracking was postulated to be responsible for the high FGR observed during transient tests. Micrographs of UO_2 specimens from the AGR/Halden Ramp Test Programme [10], which underwent power transient testing covering various power and temperature conditions, also showed separations of a fraction of the grain surfaces as well as associated grain-face gas depletion.

Models have been developed in the past to describe fission gas burst release during transients in fuel performance codes [17–21]. Generally, an additional gas release contribution from the grain boundaries during transients is introduced, considering that micro-cracking implies loss of gas storing capacity and instantaneous gas venting from cracked grain faces. The approaches from [17,18,21] consider an additional release of gas from grain boundaries due to micro-cracking, invoked when specific empirical conditions that define the transient are fulfilled. In particular, discrete thresholds are introduced in terms of power variation and absolute power. Also, a burnup-dependent temperature threshold is considered in [18,21]. The treatment proposed in [19] allows for an exponential reduction with time of the gas concentration at grain boundaries after the beginning of a transient. Based on a time- and temperature-dependent exponential function, the model from [20] considers release of a fraction of the pre-transient gas inventory above a certain temperature threshold. The model by Hering [17] allows also for the healing process of micro-cracks. Specifically, a restoration of the gas storing capacity of cracked grain faces after the transient event is considered, and is described as linear with burnup. More recently, the present authors developed a new semi-empirical model for transient gas release due to grain-boundary micro-cracking in oxide fuel [22]. Such capability is thought as an extension for purely diffusion-based models that introduces the effect of micro-cracking on local gas retention capacity of the fuel. Based on experimental evidence, the model includes a dependency upon temperature variations that results in higher FGR during transients. Compared to previous ones, this model overcomes the usage of discrete thresholds in power and/or temperature for triggering an additional release contribution. This allows for a continuous kinetics of FGR, which is a more physically sound representation. Furthermore, as the underlying mechanisms of local gas retention and release are described directly, the model preserves the physical coupling between FGR and gaseous swelling. This model has been further improved in [23] by introducing an explicit dependency of grain-boundary micro-cracking on fuel burnup, consistent with experimental observations. The present paper presents applications of this recently developed transient fission gas behaviour model in fuel rod analysis, with the aim to assess the predictive capability of the model through comparisons to experimental data and to results of purely diffusion-based models.

In order to apply a physical model such as a FGB model to integral fuel rod calculations and perform validation against integral data (e.g., fuel rod FGR), implementation in a more complex framework represented by a fuel performance code is needed. A consequence is that the accuracy of model predictions depends not only on the intrinsic characteristics of the model itself but also on calculated variables of the code (e.g., local temperature) that are input for FGB calculations. However, the calculated temperature distribution depends upon the whole thermo-mechanical modelling (including the feedback from the FGB model) and in general by the structure of the fuel performance code. Uncertainties exist that ensue from material data and physical models, but also from the basic structure of the code with the relative simplifications in representing the actual domain (e.g., dimensionality) and solving the thermo-mechanics equations (e.g., numerical technique) [24]. Recently, international benchmarks of fuel performance codes [25,26] pointed out the difficulties in predicting FGR and fuel dimensional changes due to swelling, and demonstrated that, given identical conditions, different codes can provide a broad range of outputs.

It follows that, when assessing the predictions of a specific physical model incorporated in a fuel performance code, the information inevitably contains an unknown bias associated with uncertainties in the global thermo-mechanical analysis that interacts with the model. In other words, it is difficult to evaluate the source of the deviation between the code results and the experimental data, or of an improvement in predictions obtained with a new model. Improvements may indeed arise from a better representation of the specific process, but also from compensating errors between the physical model and code's calculated global variables that are input for the model.

A way to increase the confidence in the assessment of a physical model in fuel rod analysis is applying the same model in multiple structurally different codes. Comparisons between predictions from the model applied in different codes would isolate, to some degree, the effect of the specific model from compensations related to the uncertainties in the global fuel rod analysis. This adds value to validation and confidence in conclusions drawn about the predictive capability of the specific physical model.

In the present work, we introduce this approach to model assessment and apply it to the transient FGB model from [22,23]. We implemented this model into two structurally different fuel performance codes, namely, the BISON code of Idaho National Laboratory [27] and the TRANSURANUS code developed at the Joint Research Centre in Karlsruhe [28]. These codes perform the thermo-mechanical analysis according to different approaches. Hence, given the same input and boundary conditions, the calculated global variables (e.g., temperature) from the two codes may lie in different areas of the uncertainty ranges. The FGB models of BISON [29,30] and TRANSURANUS [31,32] share a common basis and are both purely diffusion-based in their canonical forms. Also, both ac-

count for the inherent coupling between FGR and gaseous swelling. In this work, the same transient release model is implemented in the two codes as an extension of the canonical FGB models. Several light water reactor (LWR) fuel rod irradiation experiments are simulated with both codes and results of FGR are compared to experimental data in order to assess the predictive capability of the transient model.

The outline of the paper is as follows. Section 2 presents modelling of fission gas behaviour in this work, including BISON and TRANSURANUS canonical, diffusion-based models and the specific transient capability that is implemented in both codes. Section 3 provides a brief description of the two fuel performance codes. Section 4 reports on the simulated fuel rod experiments. Section 5 gives an account of the settings employed in both codes for the simulations. In Section 6, we present and discuss the results of the simulations. Conclusions are drawn and perspectives are discussed in Section 7.

2. Fission gas behaviour modelling

This Section presents the fission gas behaviour models implemented in the BISON and TRANSURANUS fuel performance codes and employed in our simulations. Both codes include diffusion-based models for the concurrent calculation of the coupled fission gas release and swelling [30,32]. These models share the same fundamental concepts, which are overviewed in Section 2.1. More details of the diffusion-based models in the two codes can be found in [29–32]. Section 2.2 reviews the transient model developed to account for the burst release effect [22,23]. This is implemented in the same form in both BISON and TRANSURANUS as an extension of the canonical, diffusion-based models.

2.1. Diffusion-based model

Fission gas transport from within the fuel grains (assumed to be spherical) to the grain boundaries is computed via numerical solution of the diffusion equation in spherical geometry

$$\frac{\partial \mathrm{C_{ig}}}{\partial t} = \frac{b}{b+g} D_s \nabla^2 \mathrm{C_{ig}} + \beta \tag{1}$$

where $\mathrm{C_{ig}}$ (at $\mathrm{m^{-3}}$) is the intra-granular gas concentration (both as single atoms and gas in bubbles), t (s) the time, g ($\mathrm{s^{-1}}$) the rate of gas atoms trapping into intra-granular bubbles, b ($\mathrm{s^{-1}}$) the rate of gas atom resolution from bubbles back into the lattice, D_s ($\mathrm{m^2\ s^{-1}}$) the intra-granular single atom diffusion coefficient, and β (at $\mathrm{m^{-3}\ s^{-1}}$) the gas generation rate. The term $b/(b+g)\ D_s$ represents the effective intra-granular diffusion coefficient according to Speight [33].

The grain-boundary gas behaviour analysis entails a physics-based and consistent treatment of both fission gas swelling and release through a direct description of the grain-face bubble development. The major features of the analysis are the following:

- The absorption rate at the grain-face bubbles is assumed to be equal to the arrival rate of gas at the grain boundaries [1,4].
- An initial number density of grain-face bubbles is considered, and further nucleation during irradiation is neglected (one-off nucleation, e.g., [5]).
- All grain-face bubbles are considered to have, at any instant, equal size and equal lenticular shape of circular projection with semi-dihedral angle of 50° [4,34].
- Grain-face bubbles grow (or shrink) by inflow of gas atoms from within the grains and concomitant absorption (or emission) of vacancies from the grain boundaries. Bubble size is also affected (reduced) by the gas escape term as FGR occurs.

The gas atom inflow rate is obtained solving Eq. 1, while the absorption/emission rate of vacancies at the bubbles is derived from the model of Speight and Beere [35]. A notable difference between the models in the two codes considered in this work is that the effect of hydrostatic stress on bubble growth (hence, the coupling of swelling and release with fuel stress) is considered in TRANSURANUS, whereas this characteristic is not available in BISON at this time.

Grain-face bubble coalescence is considered through an improved model of White [5,32]. The time derivative of the bubble number density, $\mathrm{N_{gf}}$ ($\mathrm{m^{-2}}$), due to coalescence, is calculated as a function of the time derivative of the bubble projected area on the grain face, $\mathrm{A_{gf}}$ ($\mathrm{m^2}$). The total relative volume of the lenticular grain-face bubbles represents the grain-boundary contribution to fission gas swelling [36].

In this model, thermal fission gas release is considered as a consequence of bubble growth and interconnection, and is represented based on a principle of grain face saturation. More precisely, when the fractional coverage, $\mathrm{F = N_{gf} A_{gf}}$ (/), attains a fixed saturation value, $\mathrm{F_{sat}}$, further bubble growth is compensated by gas release from the grain faces in order to maintain the saturation coverage condition:

$$\frac{\mathrm{dF}}{\mathrm{d}t} = 0 \qquad \text{if } \mathrm{F = F_{sat}} \tag{2}$$

The constant saturation coverage, $\mathrm{F_{sat}}$, value is equal to 0.5 [5,32]. Note that fission gas release and swelling are therefore described as inherently coupled phenomena, as fission gas release from the grain faces counteracts bubble growth and thereby fission gas swelling.

2.2. Transient model

An extension of the diffusion-based model outlined in Section 2.1 has been developed to introduce the burst release effect during transients [22,23]. This extension is identical in BISON and TRANSURANUS.

The transient model is developed based on the available experimental evidence of transient fission gas release in oxide fuel. From relevant experimental work reported in [6–16,37,38], the following common characteristics of the process emerge:

1. FGR during transients is characterized by a rapid kinetics (burst release).
2. Burst release is triggered by temperature variations.
3. Burst release occurs during both heating and cooling transients.
4. Burst release occurs in a limited temperature range, with the maximum release rate around a certain temperature.

As for the underlying mechanism of burst release, as discussed in Section 1, experimental evidence and consensus exist towards micro-cracking along grain boundaries [6–10]. This is also consistent with characteristic (1), which indicates a non-diffusional mechanism as responsible for the process. Based on this evidence, in this work, we assume that burst release occurs through fuel micro-cracking. However, in view of the uncertainties that would affect a detailed model for the micro-cracking mechanism, we choose to develop the transient model on a largely empirical basis. The effect of micro-cracking is considered as a loss of both gas inventory (depletion) and storing capacity of cracked grain faces. Modifications in the grain-face gas inventory and storing capacity can be represented macroscopically through the fractional coverage and the saturation coverage, respectively. Gas depletion of a fraction of the grain faces is modelled as a reduction of the fractional coverage, F, which corresponds to the fraction of grain surface occupied by gas bubbles, in the sense of an average over the fuel volume associated with a macroscopic calculation point. In particular, F is scaled by a factor, f (/), which can be interpreted microscopically as the fraction of non-cracked (intact) grain faces. The reduction of the fractional coverage effectively leads to a decrease of the amount of gas retained in the fuel (and, as a consequence, of fission gas swelling) and to a corresponding increase of fission gas release. This contribution to fission gas release adds to the diffusion-interconnection mechanism considered in the model outlined in Section 2.1. The saturation coverage, $\mathrm{F_{sat}}$, corresponds to the average grain-face gas storing capacity at a given macroscopic calculation point. The value $\mathrm{F_{sat}} = 0.5$ is considered in absence of micro-craking (Section 2.1). In a microscopic sense, we consider the grain-face gas storing capacity to become zero for a cracked grain face. Then, the loss in average storing capacity due to micro-cracking is represented in the model by scaling the saturation coverage, $\mathrm{F_{sat}}$, down from 0.5 by the factor f. Finally, a healing process of cracked grain faces is considered as a progressive restoration of the grain-face gas storing capacity.

It follows that, if the transient model is applied, the fractional coverage and the saturation coverage obey the following relationships:

$$\begin{cases} \frac{\mathrm{dF}}{\mathrm{d}t} = \left[\frac{\mathrm{dF}}{\mathrm{d}t}\right]_d + \mathrm{F}\left[\frac{\mathrm{df}}{\mathrm{d}t}\right]_c \\ \frac{\mathrm{dF_{sat}}}{\mathrm{d}t} = \mathrm{F_{sat}}\left(\left[\frac{\mathrm{df}}{\mathrm{d}t}\right]_c + \left[\frac{\mathrm{df}}{\mathrm{d}t}\right]_h\right) \end{cases} \tag{3}$$

where the subscript d stands for diffusion-controlled processes (Section 2.1), c for micro-cracking, and h for micro-crack healing. The initial (maximum) value for the saturation coverage, corresponding to all intact grain-faces, is $\mathrm{F_{sat,i}} = 0.5$. Hence, the transient model introduces a non-diffusional contribution to the evolution of gas at grain boundaries, which represents the effect of micro-cracking. Such contribution is considered through a generalized calculation of the fractional coverage and saturation coverage parameters relative to the purely diffusion-based model. In particular, the fractional coverage and saturation coverage are effectively reduced to represent the fact that a fraction of the grain faces become unable to retain any gas as micro-cracking occurs. In the following subsections, the formulations of the micro-cracking and healing terms in Eqs. 3 is detailed.

2.2.1. Effect of micro-cracking

To characterize the micro-cracking mechanism, we define an empirically based micro-cracking parameter, as detailed below. We also make the theoretical consideration that micro-cracking can only affect intact grain faces, and write

$$\left[\frac{\mathrm{df}}{\mathrm{d}t}\right]_c = -\frac{\mathrm{dm}}{\mathrm{d}t}\mathrm{f} \tag{4}$$

where f (-) is the fraction of intact grain faces, $[\mathrm{df}/\mathrm{d}t]_c$ the rate of change of f due to micro-cracking, and m (-) the micro-cracking parameter. Considering the initial conditions $\mathrm{f}(t_0) = \mathrm{f_0}$ and $\mathrm{m}(t_0) = \mathrm{m_0}$, the analytic solution of Eq. 4 is

$$\mathrm{f}(t) = \mathrm{f_0}\exp\left(-\left(\mathrm{m}(t) - \mathrm{m_0}\right)\right) \tag{5}$$

The functional form of m is chosen as a temperature-dependent sigmoid function.

Based on the available experimental evidence, the following expression for m is developed [22]

$$\mathrm{m(T)} = 1 - \left[1 + \mathrm{Q}\exp\left(\mathrm{s}\frac{\mathrm{T} - \mathrm{T_{infl}}}{\mathrm{B}}\right)\right]^{-\frac{1}{\mathrm{Q}}} \tag{6}$$

where T (K) is the local temperature, $\mathrm{T_{infl}}$ (K) the value for the temperature at the inflection point of the function m (T) (inflection temperature), and B (K) and Q (-) are parameters related to the temperature-domain width of the phenomenon and the deviation from symmetric behaviour during heating/cooling transients, respectively. The values B = 10 K and Q = 33 [22,23] are used. We also investigated the sensitivity of model predictions to parameters through a sensitivity analysis (Section 2.2.3), demonstrating that the sensitivity of results to Q and B is low

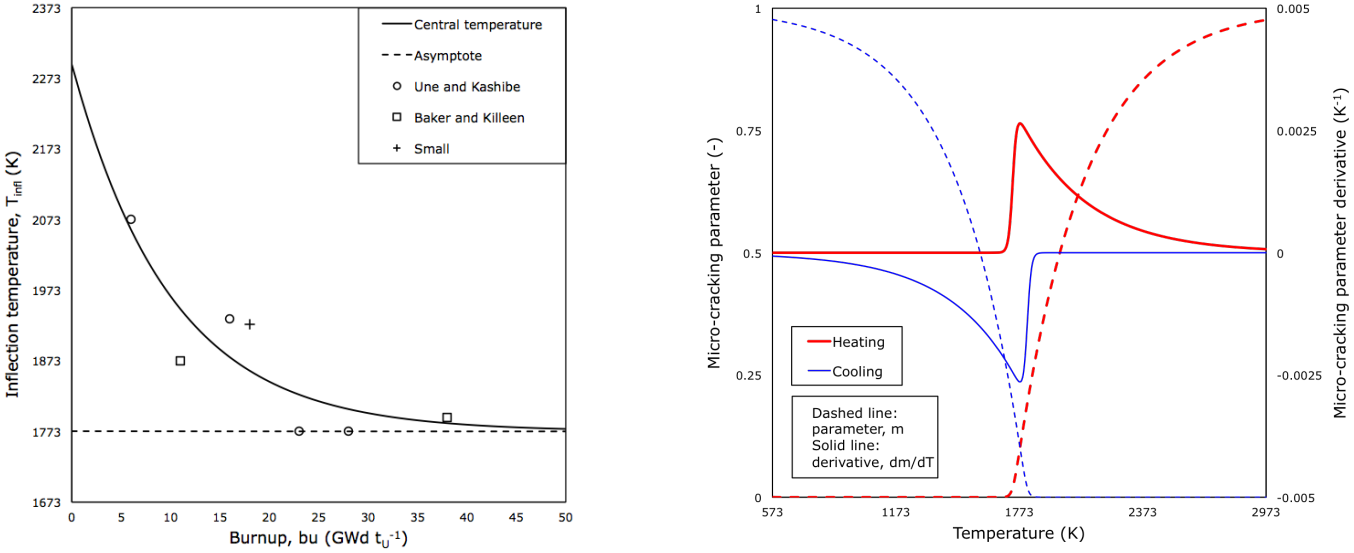

Figure 1: Left: Experimental data for the temperature of maximum burst release rate from Une and Kashibe [13], Baker and Killeen [37] and Small [38] as a function of burnup and best-estimate fitting curve. Right: Micro-cracking parameter, m, and temperature derivative, dm/dT , as a function of temperature. The asymptotic value of 1773 K for the inflection temperature is considered for this plot.

compared to T_{infl}. Equation 4 combined with the formulation for m (Eq. 6) implies

$$\left[\frac{df}{dt}\right]_c = 0 \qquad \text{if} \quad \frac{dT}{dt} = 0 \tag{7}$$

which conforms to the experimentally observed characteristic (2) of burst release as triggered by temperature variations [13,16,37,38]. The value of s (-) in Eq. 6 is set to +1 during heating transients and to −1 during cooling transients, so that m increases during both heating and cooling, in conformity with experimental observations (characteristic 3). According to Eq. 6, the absolute value of the temperature derivative for m is maximum at T_{infl} (see also Fig. 1, right), thus the combined Eqs. 4, 6 reproduce the maximum rate of burst release at T_{infl} as temperature varies in time. Hence, the present model with the so constructed micro-cracking parameter also allows for characteristic (4) of the process.

The concept of a temperature of maximum burst release rate, or inflection temperature, is corroborated by experimental work from [13,16,37,38], showing peaks of release rate occurring as the fuel reaches a certain temperature, and exhausting within a limited temperature range. Moreover, the experiments indicate that a dependency exists of the inflection temperature on fuel burnup. For the calculation of the parameter T_{infl} in the model, the following correlation is used

$$T_{infl} = \alpha + \beta \exp\left(-\frac{bu}{\gamma}\right) \tag{8}$$

where α = 1773 K, β = 520 K, γ = 10 GWd t_U^{-1}, and bu (GWd t_U^{-1}) is the burnup at current time step. Equation 8 is derived from the best-estimate fit of quantitative experimental data (Fig. 1, left).

The micro-cracking parameter, m, and the temperature derivative, dm/dT , are reported in Fig. 1 (right) for a value of T_{infl} = 1773 K. The inflection point (maximum absolute value of derivative) for m at T_{infl} corresponds to the maximum rate of burst release at the inflection temperature. The asymmetry around the inflection point conforms to experimental observations indicating that burst release during heating transients is higher in the temperature region above the inflection temperature than below, and conversely [12].

A physically based description of micro-cracking would take into account localized stresses at grain boundaries. Here, we choose to adopt an empirical description in consideration of the uncertainties involved in the calculation of localized stresses, which may outweigh the improved accuracy from the added physical detail [21]. Rather than being an attempt to capture the complex underlying physics of burst release, the transient model represents a pragmatic approach to allow for this important aspect of FGB in fuel performance codes in an effective way. Nevertheless, the empirical basis of the model entails limitations in terms of flexibility of application and insight into the underlying physical processes. Further developing the present preliminary approach to a more physically-based description is advisable in perspective in order to further improve model predictivity.

2.2.2. Effect of micro-crack healing

The effect of micro-crack healing is accounted for in the model via an empirical treatment. Following Hering [17], the effect of the healing process is represented as a pro-

gressive restoration with time of the gas storing capacity of cracked grain faces and is purely burnup-dependent. Analogous to the treatment of micro-cracking (Section 2.2.1), to characterize the process we define a micro-crack healing parameter, u (-). We also observe that the mechanism can only affect cracked grain faces, and write

$$\left[\frac{\mathrm{df}}{\mathrm{d}t}\right]_h = \frac{\mathrm{du}}{\mathrm{d}t}\left(1-\mathrm{f}\right) \tag{9}$$

where $[\mathrm{df}/\mathrm{d}t]_h$, is the rate of change of the fraction of intact grain faces, f, due to micro-crack healing. The healing parameter is taken as a function of fuel burnup, i.e., $\mathrm{u} = \mathrm{u}\left(bu\left(t\right)\right)$. With the initial conditions $\mathrm{f}\left(t_0\right) = \mathrm{f}_0$ and $\mathrm{u}\left(t_0\right) = \mathrm{u}_0$, the analytic solution of Eq. 9 is

$$\mathrm{f}\left(t\right) = \mathrm{f}_0 + \left(1-\mathrm{f}_0\right)\left[1-\exp\left(\mathrm{u}\left(t\right)-\mathrm{u}_0\right)\right] \tag{10}$$

The functional form of the healing parameter is

$$\mathrm{u}(bu) = \frac{bu}{\tau} \tag{11}$$

where $\tau = 1$ GWd $\mathrm{t_U}^{-1}$ [17,23].

2.2.3. Analytic sensitivity analysis of the transient model

In order to assess the sensitivity of calculations to model parameters, we perform an analytic sensitivity analysis of the developed representation of the the micro-cracking effect, in particular, Eq. 6. The model parameters of interest in this sensitivity analysis are B, Q, $\mathrm{T_{infl}}$ (Section 2.2.1). As representative figure of merit, the fractional coverage, F, is selected. The reason for this selection is the fractional coverage being the physical quantity that carries the information from the transient model to the overall FGB model through Eq. 3.

Table 1 reports the definitions and the analytic expressions of the sensitivity coefficients (k_T, k_B, and k_Q) as defined in this analysis for the three parameters of interest ($\mathrm{T_{infl}}$, B, Q, respectively). The results of the analysis are reported in Fig. 2. The sensitivity coefficient k_T, associated with the parameter $\mathrm{T_{infl}}$, is characterized by the higher average and maximum over the considered temperature and burnup range (Fig. 2a). Hence, it clearly emerges from the sensitivity analysis that $\mathrm{T_{infl}}$ is the dominant parameter. Fig. 2b shows the temperature-burnup 2D map of the k_T sensitivity coefficient, which is maximum close to the value of $\mathrm{T_{infl}}$ and rapidly drops away from it. This is consistent with the fractional coverage (hence, the overall FGB model results) being significantly affected by the transient model only in the neighbourhood of the inflection temperature (Eqs. 3-6). Instead, the sensitivity of the figure of merit to the B and Q parameters is low (coefficients k_B and k_Q, respectively, in Fig. 2a), which points out that the choice of the values for Q and B has a limited impact on model predictions.

3. Fuel performance codes

Several fuel rod irradiation experiments are simulated in this work using the BISON and TRANSURANUS fuel performance codes with the FGB models described in Section 2. In this Section, the main features and capabilities of the two codes are briefly overviewed.

3.1. The BISON code

BISON [27] is a finite-element based nuclear fuel performance code developed at the Idaho National Laboratory (INL, USA). The code can be applied to steady-state and transient fuel simulations, and allows for 1D spherically symmetric, 2D axisymmetric or generalized plane strain, or 3D geometry representations. BISON's governing relations consist of fully-coupled partial differential equations for species conservation and thermo-mechanics, and include constitutive laws for nonlinear kinematics and nonlinear material behaviour. Models are available to describe the various interacting processes involved in fuel rod behaviour. Details can be found in [27,29,39]. In the present work, we chose to represent the fuel rods analysed by BISON with 2D axisymmetric models. Also, the pellet stack is represented as a smeared fuel column. An example of BISON computational mesh used for the present simulations is reported in Fig. 3a.

3.2. The TRANSURANUS code

TRANSURANUS [28] is an integral fuel performance code developed at the Joint Research Centre – Karlsruhe (Germany). The code approximates the fuel rod behaviour with an axisymmetric, axially-stacked, one-dimensional radial representation (often referred to as 1.5D). The code can be employed for both steady-state and transient analyses, and incorporates models accounting for the different and interrelated phenomena occurring in the fuel rod. Details can be found in [28,31]. In TRANSURANUS, the fuel rod is discretised in axial slices, or sections, and in radial coarse zones for the evaluation of the material properties. The coarse zones are in turn divided into finer zones to perform the numerical integrations needed for the thermo-mechanical analysis. A schematization of the fuel rod discretisation adopted by TRANSURANUS is shown in Fig. 3b.

4. Fuel rod irradiation experiments

For the analyses with the BISON and TRANSURANUS codes, we considered 19 LWR fuel rod irradiation experiments from the OECD/NEA International Fuel Performance Experiments (IFPE) database [15]. The power histories of the selected experiments are comprised of a base irradiation under normal operating conditions followed by a ramp test at high power. The considered cases are listed in Table 2. Some features of the fuel rods are also summarized, focusing on data that are directly related to

Table 1: Definitions and analytic expressions of the relative sensitivity coefficients defined in this analysis. The analytic expressions can be derived by differentiation from Eqs. 3, 4 and 6.

Parameter	Relative sensitivity coefficient	Definition	Analytic expression
T_{infl}	k_T	$\frac{dF}{F} = k_T \frac{dT_{infl}}{T_{infl}}$	$k_T = f \frac{s}{B} T_{infl} \exp\left(s\frac{T-T_{infl}}{B}\right)\left[1+Q\exp\left(s\frac{T-T_{infl}}{B}\right)\right]^{-\frac{1}{Q}-1}$
B	k_B	$\frac{dF}{F} = k_B \frac{dB}{B}$	$k_B = k_T \frac{T-T_{infl}}{T_{infl}}$
Q	k_Q	$\frac{dF}{F} = k_Q \frac{dQ}{Q}$	$k_Q = -fQ\exp\left(-\frac{1}{Q}\log\left(1+\exp\left(s\frac{T-T_{infl}}{B}\right)\right)\right) \cdot \left[\frac{1}{Q^2}\log\left(1+\exp\left(s\frac{T-T_{infl}}{B}\right)\right) - \frac{\exp\left(s\frac{T-T_{infl}}{B}\right)}{Q\left(1+\exp\left(s\frac{T-T_{infl}}{B}\right)\right)}\right]$

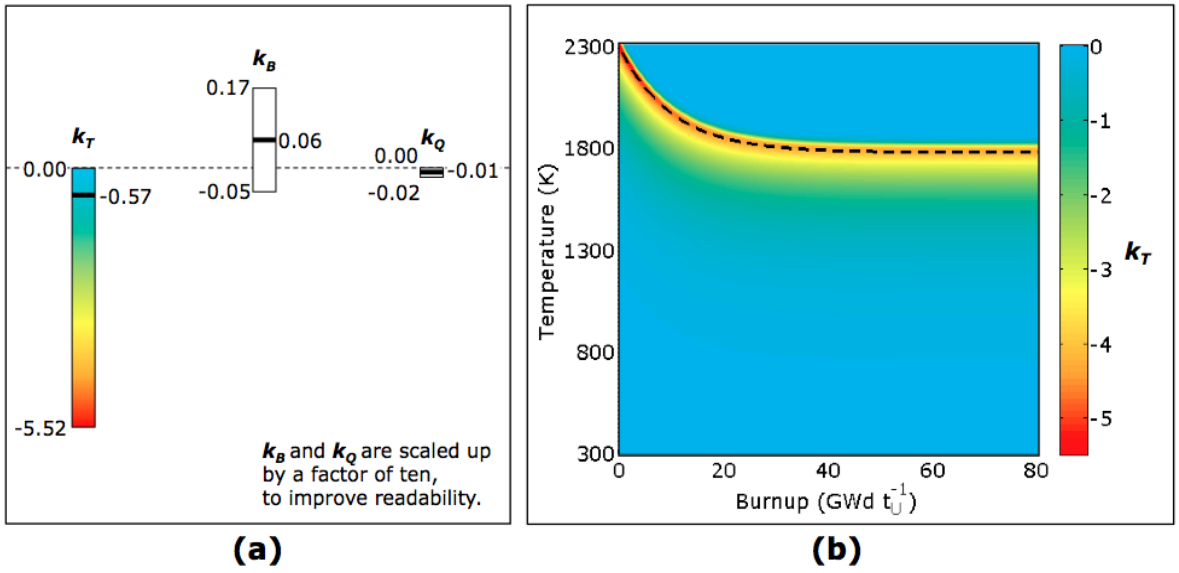

Figure 2: Results of the analytic sensitivity analysis of the transient model. (a) Bar plot reporting the upper, mean and lower value of the relative sensitivity coefficients analysed over the temperature-burnup range of [300, 2300 K] x [0, 80 GWd $t_U{}^{-1}$]. (b) Detailed temperature-burnup 2D map of the relative sensitivity coefficient associated with the inflection temperature. The dashed line represents the inflection temperature as a function of burnup. For interpretation of the references to colour in this figure legend, the reader is referred to the web version of the article.

FGB modelling. Some of these experiments were included in the IAEA Coordinated Research Projects FUMEX-II [25] and FUMEX-III [26]. We carried out the simulations coherently with the pre-irradiation characterization data, power histories and coolant conditions provided in the IFPE database. Experimental data available from these experiments include Post-Irradiation Examination (PIE) measurements of integral fuel rod FGR at the end of irradiation (generally from rod puncturing). In some cases, the time evolution of integral FGR inferred from on-line rod pressure measurements and PIE of radial xenon profiles in the fuel are also included.

5. Set-up of calculations

Calculations were performed using the BISON and TRANSURANUS codes with the relative physical models (see references in Section 3). In addition, we applied the FGB models presented in Section 2 for the calculation of fission gas release and fuel gaseous swelling.

In order to apply the FGB models, it is necessary to specify a fission gas diffusion coefficient (Eq. 1) and a fuel grain size. For the present simulations, we used the single atom diffusion coefficient based on Turnbull et al. [40] as in [30]. The intra-granular diffusion equation, Eq. 1, is solved numerically using the FORMAS algorithm from [41–43]. To obtain the initial grain radii (Table 2), the measured linear intercepts were multiplied by a factor of 0.78 [44]. Grain growth during irradiation is accounted for using the model of Ainscough et al. [45]. The AN3, AN4, II3 and IFA 597.3 experiments involved re-fabrication of the fuel rod prior to the ramp test, which is considered in the simulations by re-defining specific parameters (fill gas pressure and composition) and employing the restart capabilities of the codes.

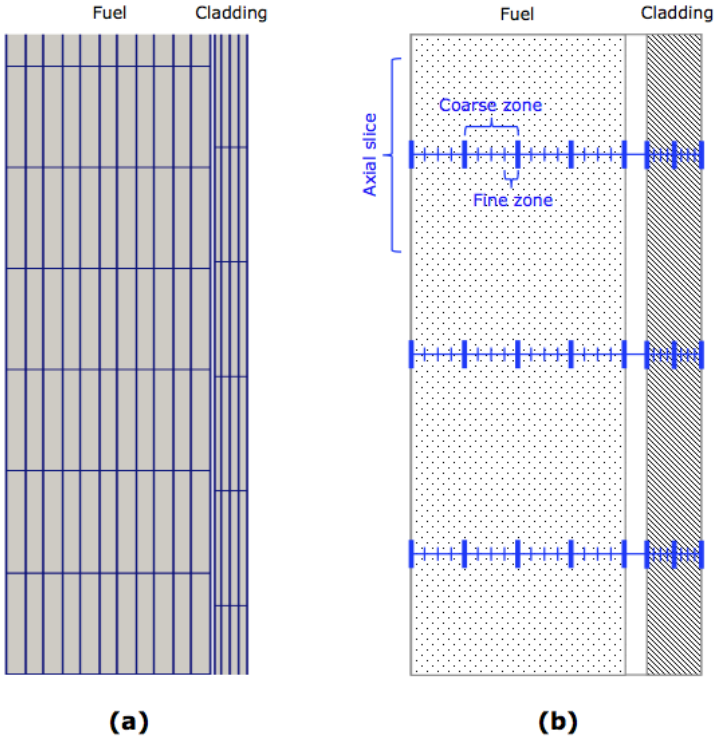

Figure 3: (a) Example of BISON 2D finite-element mesh employed in this work, and (b) representation of TRANSURANUS mesh (not to scale).

Table 2: Summary of the irradiation experiments from the OECD/NEA IFPE database [15] analysed in this work.

Fuel rod	Database	Reactor type	Average burnup ($GWd\,t_U{}^{-1}$)	FGR, measured (%)	Grain radius (μm)
PK1-1	Super-Ramp	PWR	35.4	8.5	4.68
PK1-2	Super-Ramp	PWR	35.6	13.6	4.68
PK1-3	Super-Ramp	PWR	35.2	22.1	4.68
PK1-4	Super-Ramp	PWR	33.1	13.0	4.68
PK2-1	Super-Ramp	PWR	45.2	28.0	4.29
PK2-2	Super-Ramp	PWR	45.1	32.1	4.29
PK2-3	Super-Ramp	PWR	44.6	44.9	4.29
PK2-4	Super-Ramp	PWR	41.4	9.5	4.29
PK6-2	Super-Ramp	PWR	36.8	3.5	17.16
PK6-3	Super-Ramp	PWR	36.5	6.7	17.16
PK6-S	Super-Ramp	PWR	35.9	6.1	17.16
AN2	Risø-3	PWR	43.2	29.7	4.68
AN3	Risø-3	PWR	44.0	35.5	4.68
AN4	Risø-3	PWR	44.1	40.9	4.68
AN8	Risø-3	PWR	43.2	13.7	4.68
GE7	Risø-3	BWR	41.7	14.4	9.4
II3	Risø-3	BWR	16.3	17.4	9.5
Rod 8	IFA 597.3	BWR	70	15.8	6.1
L10	Regate	PWR	53.4	10.2	7.5

6. Results and discussion

In this Section, we present the assessment of the transient FGB model through analysis of the 19 LWR fuel rod irradiation experiments presented in Section 4. We simulated each fuel rod with both the BISON and TRANSURANUS codes. Also, each fuel rod is analysed both using the canonical diffusion-based models (Section 2.1) alone and with the transient (burst release) model extension applied. First, in Section 6.1, detailed results for two selected

cases is presented, including time evolution of FGR and local xenon concentrations across the fuel pellets. Then, in Section 6.2, the results of integral fuel rod FGR at the end of irradiation for the overall set of considered cases are presented and compared to the experimental data. The integral FGR is defined as the ratio of the released to generated gas in the fuel rod. The integral FGR is generally the quantity of interest to engineering-scale fuel modelling, as it corresponds to the total amount of gas released to the fuel rod free volume.

6.1. Detailed results for the Risø-3 AN3 and AN4 simulations

The Risø-3 AN3 and AN4 fuel rods were equipped with a fuel centreline thermocouple and a pressure transducer in the plenum, so that the time evolution of FGR could be inferred based on the on-line pressure measurements. Moreover, PIE data for the diametric xenon concentration profiles are available for these two experiments. In particular, the diametric profile of the total xenon concentration (summation of intra-granular and inter-granular contributions) was determined by X-Ray Fluorescence (XRF) analysis. Hence, these experiments allow for a detailed investigation of model fidelity, since comparisons of calculations to time-dependent fuel rod FGR (as opposed to the sole end-of-irradiation values) as well as retained gas in the fuel as a function of diametric position in the fuel pellet are possible.

Figure 4 shows results from the BISON and TRANSURANUS calculations along with experimental measurements of integral FGR during the AN3 ramp test. Measured and calculated fuel central temperature is also shown. As illustrated in the figures, burst release during transients is experimentally observed during the AN3 test (note the stepwise release at about 48 and 70 hours from the beginning of the test). Results point out a significant improvement in FGR predictions with the transient model compared to the canonical diffusion-based models (w/o transient model), for both codes. Improvements are in terms of both representation of the FGR kinetics and end-of-irradiation FGR values. In particular, differently from the canonical models, the transient model accounts for the burst release effect, with stepwise release during transients being reproduced. However, the magnitudes of the experimental (from pressure measurements) and calculated FGR steps are different, with an under-prediction being observed. Indeed, part of the rapid increase in the measured inner pressure and FGR may be ascribed to a delayed detection of gas actually released before the transient and related to gap and cracks reopening during power reductions [46]. Such hypothesis may partly explain these discrepancies. When the transient model is used, the deviation between the end-of-irradiation FGR calculated with both codes and the measured one appears satisfactory, in view of the intrinsic modelling uncertainties [30]. With the canonical models, burst release is not reproduced, indicating that the phenomenon cannot be represented through a purely diffusion-based interpretation of fission gas behaviour.

Figure 5 shows results from the BISON and TRANSURANUS calculations along with experimental measurements of fuel central temperature and integral FGR during the AN4 ramp test. Significant improvements of the FGR predictions are observed when applying the transient model compared to the canonical models, for both codes. Also in this case, improvements are both in the predicted kinetics of the process and the end-of-irradiation FGR value.

From the presented results, it is noted that the calculated FGR with the canonical models (w/o transient model) from the two codes is significantly different, with BISON tending to compute a higher FGR than TRANSURANUS. Also, the impact of the transient model on predictions is different. It is postulated that this would be ascribed to the effect of compressive hydrostatic stress. In the canonical FGB model of TRANSURANUS, hydrostatic stress acts to compress grain-face bubbles, delaying the saturation of the grain faces [1,32,35] and reducing FGR. This effect is currently neglected in BISON [29]. Correspondingly, in the TRANSURANUS canonical representation, a higher amount of gas is retained in the fuel compared to BISON. Hence, more gas is available for release via micro-cracking at the grain faces, which is considered if the transient model is applied. This peculiarity will be the subject of further investigation once a stress-dependent FGB model is included in BISON. Other contributions to differences between predictions from the two codes include differences in the calculated fuel temperatures, as well as some differences between the formulations of the canonical FGB models of the codes [29–32].

In the analysis of both AN3 and AN4 experiments, we compare the temperature calculated by the codes with the measured temperature during the ramp tests. Calculations with the transient FGB model applied are considered. For both the BISON and TRANSURANUS simulations, the results point out a good agreement between calculated and experimental temperatures for the AN3 experiment. As for the AN4 experiment, the deviation between the calculated temperatures and the experimental data is more significant. However, for both BISON and TRANSURANUS the error is within 10% of the experimental values, which is in line with the intrinsic uncertainties [27,28].

Finally, we present comparisons of calculations to experimental data of local xenon concentrations in the fuel. In particular, we consider profiles of retained xenon concentration across the pellet diameter, measured by XRF analysis in a fuel sample[1] obtained from the AN3 rod [15,47]. The comparisons between the experimental profile and the BISON and TRANSURANUS calculations, both

[1]This fuel sample is referred to as CB-2R-5. The sample was obtained by transverse cutting of the AN3 rod. It has an estimated local burnup of 46.0 $\mathrm{GWd\,t_U{}^{-1}}$ and an estimated maximum linear heat rate of 41.3 $\mathrm{kW\ m^{-1}}$ [15,47].

with the canonical diffusion-based models and with the transient model extension applied, are illustrated in Fig. 6. The plots showcase local gas retention in the fuel, which is coupled to gas release, as reproduced by the fission gas behaviour models in the codes. Direct modelling of the physical mechanisms of fission gas diffusion and bubble evolution underlies calculated concentrations [30,32]. The transient model acts on such physical representation introducing a reduction, dependent on local conditions, of the retained gas concentration. This affects (reduces) local fuel gaseous swelling and leads to a corresponding increase in FGR. In general, a good agreement is observed between the calculated and the measured xenon concentration profiles, although some discrepancies are observed. These may be ascribed to uncertainties inherent in fission gas behaviour modelling [30], as well as uncertainties in the measured concentrations, which are associated with the experimental technique [48]. For both codes, the tran-

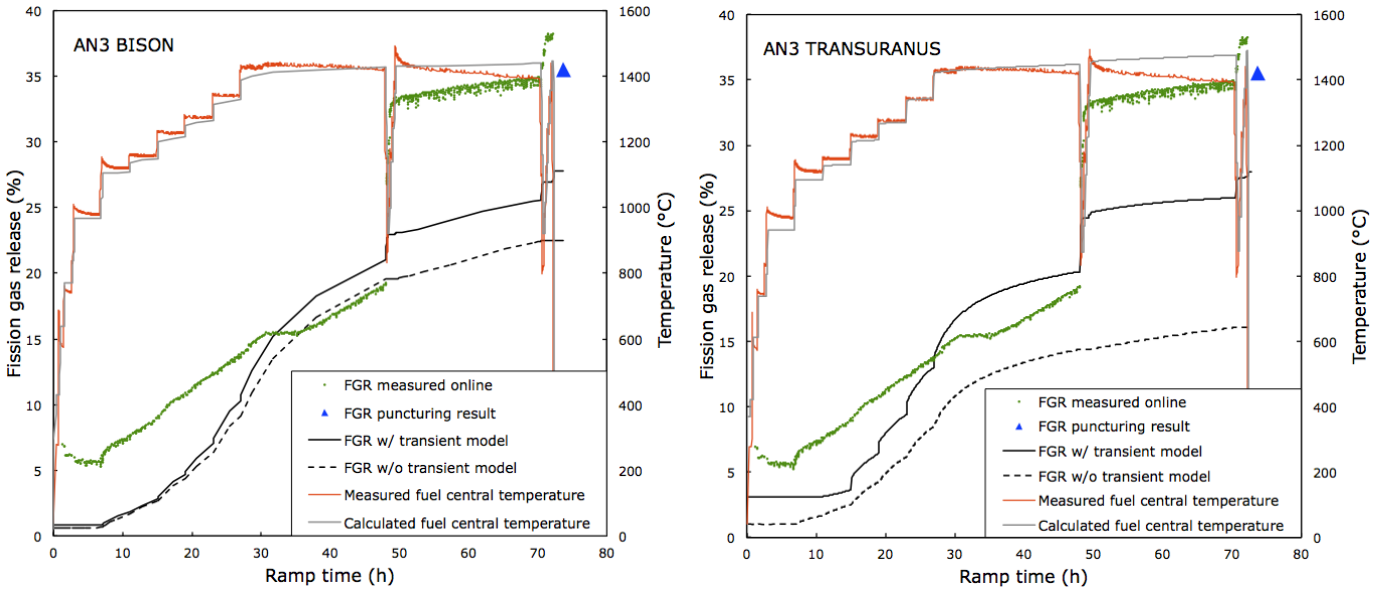

Figure 4: FGR and fuel central temperature as a function of time for the AN3 fuel rod during the ramp test. Experimental measurements are compared to calculations with BISON (left) and TRANSURANUS (right). FGR results obtained with (w/) and without (w/o) the transient model applied are presented. For interpretation of the references to colour in this figure legend, the reader is referred to the web version of the article.

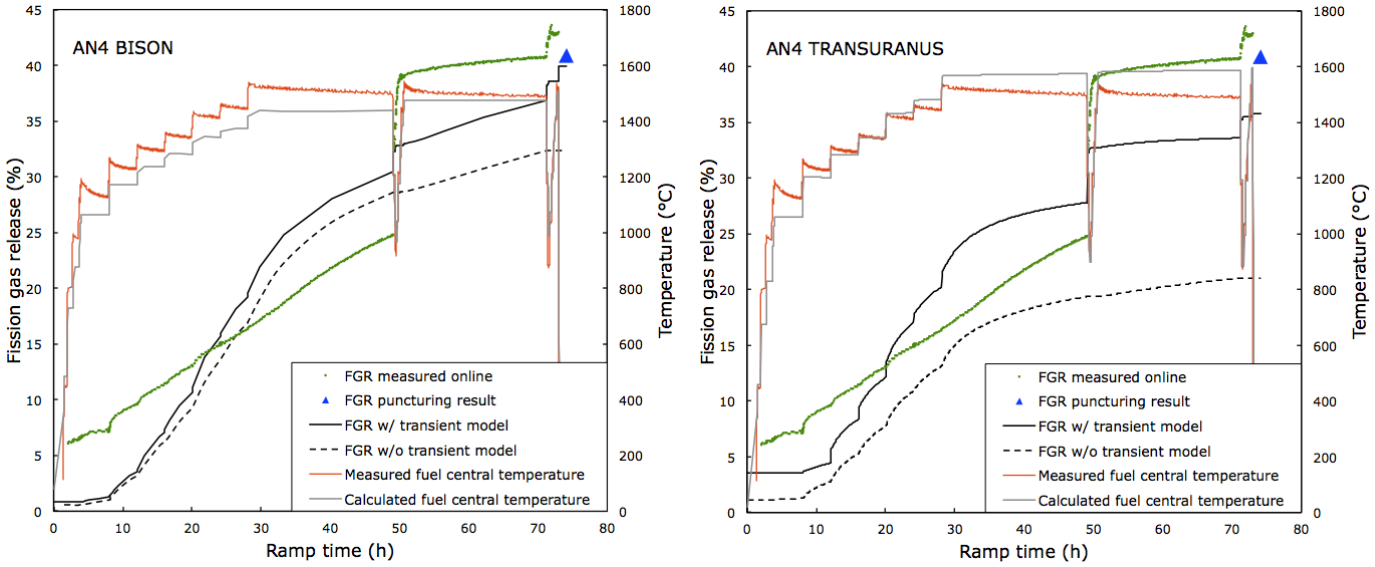

Figure 5: FGR and fuel central temperature as a function of time for the AN4 fuel rod during the ramp test. Experimental measurements are compared to calculations with BISON (left) and TRANSURANUS (right). FGR results obtained with (w/) and without (w/o) the transient model applied are presented. For interpretation of the references to colour in this figure legend, the reader is referred to the web version of the article.

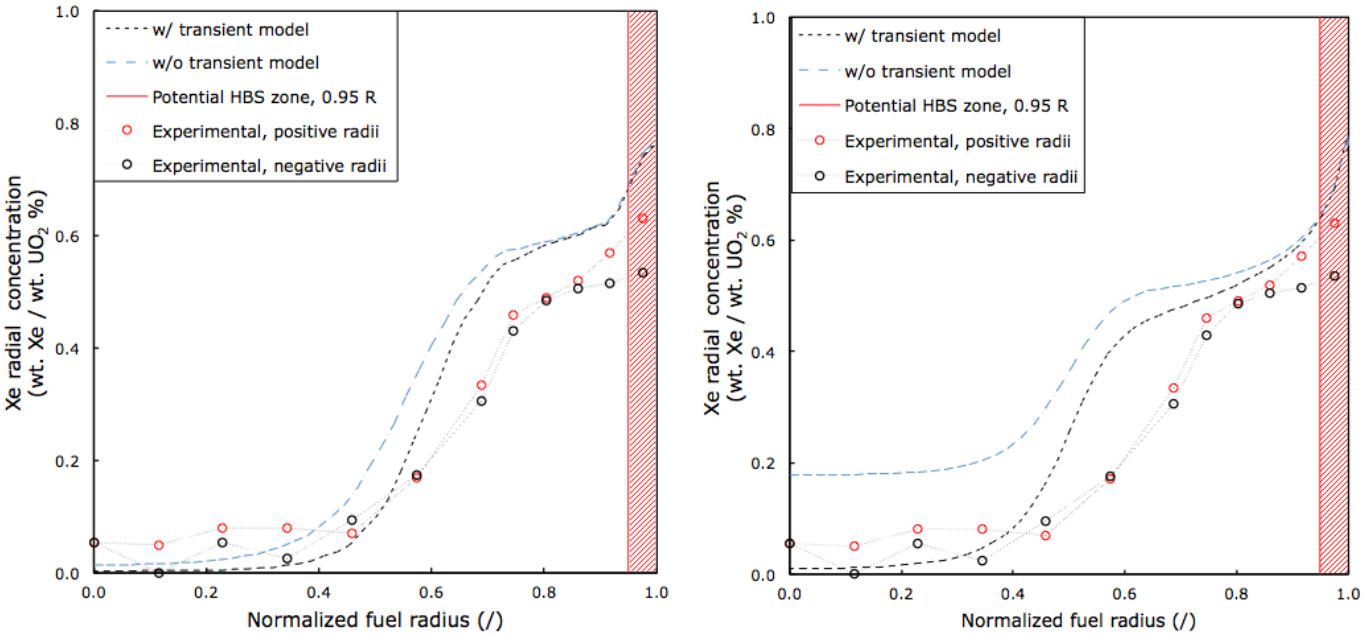

Figure 6: Radial profiles of xenon concentration in the CB-2R-5 fuel sample from the AN3 rod. Experimental data are compared to calculations with BISON (left) and TRANSURANUS (right). Since the experimental data were measured along the fuel diameter, but our calculations are axially symmetric, we define a positive and a negative radius in reporting measurements. The origin is assumed in the centre of the pellet. The red region represents the potential HBS formation zone, which is not accounted for in the simulation and for which the comparison is less meaningful. For interpretation of the references to colour in this figure legend, the reader is referred to the web version of the article.

Table 3: Summary of integral FGR results obtained with BISON and TRANSURANUS for the fuel rod irradiation experiments analysed in this work.

Fuel rod	**FGR (%), measured**	**BISON**		**TRANSURANUS**	
		FGR (%), w/o transient model	FGR (%), w/ transient model	FGR (%), w/o transient model	FGR (%), w/ transient model
PK1-1	8.5	5.6	8.1	6.7	14.2
PK1-2	13.6	8.4	11.8	9.0	18.0
PK1-3	22.1	14.4	18.5	13.2	24.0
PK1-4	13.0	12.6	16.5	12.2	22.0
PK2-1	28.0	8.8	12.6	10.0	19.0
PK2-2	32.1	16.9	22.3	15.9	27.5
PK2-3	44.9	23.5	28.2	19.0	31.9
PK2-4	9.5	2.1	5.0	5.7	14.9
PK6-2	3.5	0.9	1.3	0.9	2.2
PK6-3	6.7	1.3	1.8	1.3	2.8
PK6-S	6.1	0.9	1.3	0.8	2.1
AN2	29.7	23.3	26.8	15.8	28
AN3	35.5	22.5	27.8	16.2	28.1
AN4	40.9	32.4	39.9	21.0	35.8
AN8	13.7	6.0	8.3	7.4	16.6
GE7	14.4	8.9	12.3	6.0	11.3
II3	17.4	8.8	12.7	3.2	6.8
Rod 8	15.8	3.7	8.4	12.1	20.4
L10	10.2	3.3	6.2	3.5	8.1

sient model tends to improve the results compared to the canonical model. For the TRANSURANUS calculation with the canonical model, a higher amount of gas is stored in the fuel inner region compared to the BISON calculation. This is consistent with the differences in calculated FGR mentioned above. As discussed, such different be-

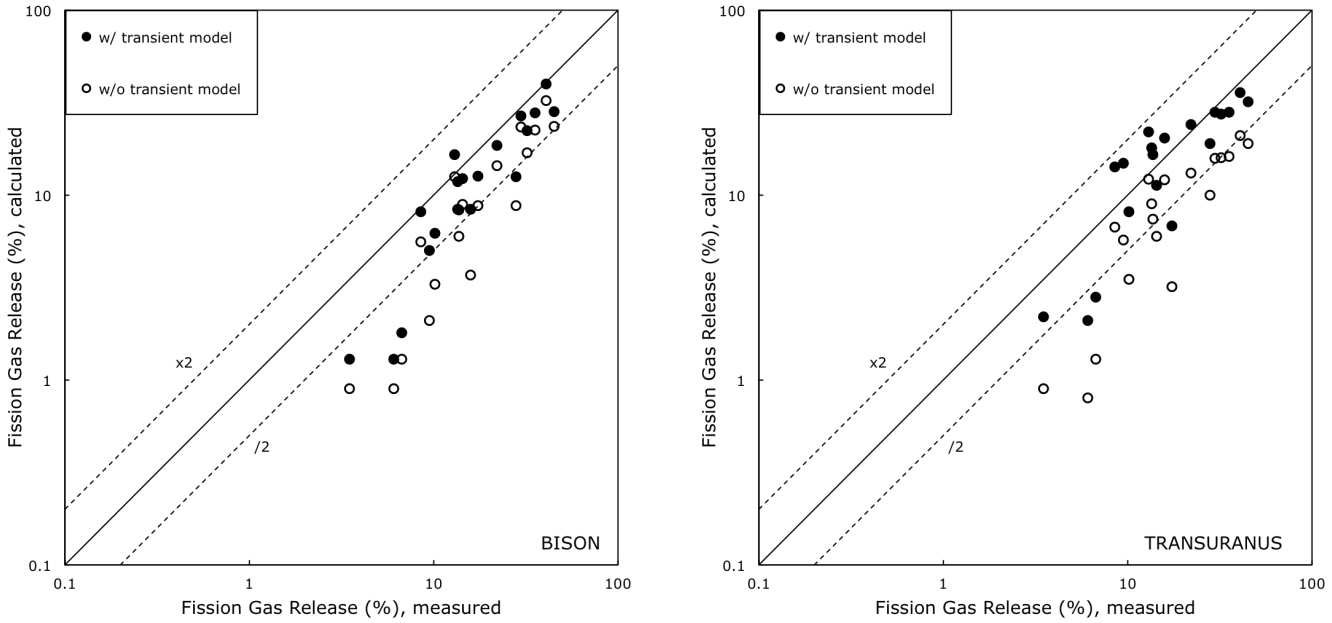

Figure 7: Simulation results of integral FGR at the end of irradiation from BISON (left) and TRANSURANUS (right) compared to experimental data. Each data point corresponds to one of the 19 irradiation experiments from the OECD/NEA IFPE database analysed in this work. The open symbols represent the results obtained with the canonical models, whereas the full symbols are the results obtained with the transient model applied. The distance from the 45° line is a measure of the accuracy. Dashed lines correspond to deviations of a factor of 2 from measured data [30].

haviour may be ascribed to the role of hydrostatic stress in compressing grain-face bubbles and limiting release, which corresponds to higher gas retention and is considered only in TRANSURANUS at this time. In the outermost region of the fuel pellet, red-marked in Fig. 6, the potential formation of the High Burnup Structure (HBS) may affect the xenon concentration profile [49,50]. Fission gas behaviour in the HBS is different than in the regular fuel structure, requiring a different modelling approach. This will be the subject of future work.

6.2. Fission gas release results for the overall set of simulations

In this Section, we present simulation results in terms of integral FGR at the end of fuel rod irradiation for all 19 experiments considered in this work (Table 2). The comparisons of calculations to experimental data are shown in Fig. 7 for BISON (left) and TRANSURANUS (right). Data are tabulated in Table 3.

In Fig. 7, both results obtained with the canonical diffusion-based models (Section 2.1) and those obtained applying the transient model extension (Section 2.2) are shown. Comparisons demonstrate that, when the transient model is applied, an improvement of the overall results is obtained for both codes. To provide a quantitative estimation of the improvement brought about by the transient model, we computed the relative error of each simulation result with respect to the measured FGR, i.e., $(\mathrm{FGR}_{\mathrm{calculated}} - \mathrm{FGR}_{\mathrm{measured}})/\mathrm{FGR}_{\mathrm{measured}}$. The average of the absolute values of this error is a measurement of the overall accuracy. With the canonical models, the average relative error over all considered cases is of about 50% and 52% for BISON and TRANSURANUS, respectively. When applying the transient model, errors reduce to approximately 35% for both codes. Hence, the transient model improves the overall predictive accuracy for both codes. Furthermore, the overall improvements for the two codes are similar.

For both BISON and TRANSURANUS calculations, the higher relative error is observed for the Super-Ramp PK6 rods. The FGR values for these cases (Table 3) are lower. In this region of lower FGR, higher relative simulation errors are indeed expected due to (i) higher inherent modelling uncertainties [30] and (ii) higher numerical errors related to the solution of the intra-granular fission gas diffusion equation with the current algorithm (Section 5) [41,51]. Recent developments on numerical modelling of fission gas diffusion can be found in [51].

7. Conclusions and perspectives

In this work, we presented and assessed a model for transient FGB in oxide fuel that accounts for the burst release process associated with fuel micro-cracking. The model conforms to the experimentally observed characteristics of the process and extends conventional diffusion-

based interpretations of FGB in fuel performance codes. We implemented the transient model in two structurally different fuel performance codes, i.e., BISON and TRANSURANUS, as an extension of the canonical, purely diffusion-based FGB models of the codes. We assessed the model by performing simulations of 19 LWR fuel rod irradiation experiments from the OECD/NEA IFPE database and comparing code predictions from both codes to the available experimental data. The simulation results pointed out an improvement of the overall FGR description by employing the transient model compared to the canonical models. More in detail:

- A better accuracy in the predictions of integral FGR at the end of irradiation was observed for both BISON and TRANSURANUS calculations. In particular, the average relative error of FGR predictions over the 19 considered cases improved from about 50% with the canonical models to approximately 35% with the transient model applied, for both codes.
- A more consistent representation of the FGR kinetics during transients was observed for both codes, as pointed out by comparisons of calculated FGR time evolution to on-line measurements for the Risø-3 AN3 and AN4 experiments. In particular, unlike simulations with the canonical models, the burst release effect was reproduced in calculations applying the transient model.
- Satisfactory capabilities of both codes in predicting diametric xenon concentration profiles were observed, as pointed out by comparison of calculations to PIE for the Risø-3 AN3 experiment. The transient model tends to improve the results of local xenon concentration compared to the canonical models.

In short, the present results indicated that the transient FGB model applied to fuel rod simulations allows for both an improved qualitative representation of the kinetics of FGR during transients and an improved quantitative accuracy of FGR predictions. Furthermore, by applying the model in two structurally different fuel performance codes, it was verified that such improvements hold for both codes. Such cross comparison provides an argument in favor of the improvements being related to the specific model itself, rather than to possible compensating errors between the model and the global fuel rod thermo-mechanical analysis. The successful outcome of model assessment in two different fuel performance codes thus suggests that the transient fission gas behaviour model indeed provides a better representation of the relevant physics than purely diffusion-based models. Therefore, the present work provides a meaningful contribution to validation of the transient FGB model and a valid indication that the proposed representation of burst release due to micro-cracking captures additional, relevant physics of transient FGB relative to purely diffusion-based models.

Further developments of the FGB models of BISON and TRANSURANUS should include the description of gas behaviour in the HBS, especially during transients. In addition, introducing the effect of hydrostatic stress on FGB in BISON is planned. Moreover, a description of transient fission gas release as triggered by micro-cracking, similar to the model considered in this work, could be developed also for MOX fuel if enough data become available.

Acknowledgments

The authors wish to thank Prof. A. Cammi and Dr. S. Lorenzi (Politecnico di Milano) for the fruitful discussions.

This research contributes to the Joint Programme on Nuclear Materials (JPNM) of the European Energy Research Alliance (EERA), in the specific framework of the COMBATFUEL Project.

The work is also part of the R&D activities carried out by POLIMI in the framework of the IAEA Coordinated Research Programme FUMAC.

The submitted manuscript has been authored by a contractor of the U.S. Government under Contract DE-AC07-05ID14517. Accordingly, the U.S. Government retains a non-exclusive, royalty free license to publish or reproduce the published form of this contribution, or allow others to do so, for U.S. Government purposes.

References

[1] D. R. Olander, Fundamental Aspects of Nuclear Reactor Fuel Elements, Technical Information Center – Energy Research and Development Administration, University of California, Berkeley, CA, USA, 1976.

[2] P. Van Uffelen, R. J. M. Konings, C. Vitanza, J. Tulenko, Analysis of reactor fuel rod behavior, in: D. G. Cacuci (Ed.), Handbook of Nuclear Engineering, Vol. 13, Springer Science + Business Media, LLC., New York, NY, USA, 2010, pp. 1519–1627.

[3] H. Matzke, Gas release mechanisms in UO_2 – a critical review, Radiation Effects 53 (1980) 219–242.

[4] R. J. White, M. O. Tucker, A new fission-gas release model, Journal of Nuclear Materials 118 (1983) 1–38.

[5] R. J. White, The development of grain-face porosity in irradiated oxide fuel, Journal of Nuclear Materials 325 (2004) 61–77.

[6] R. M. Carroll, J. G. Morgan, R. B. Perez, O. Sisman, Fission density, burnup, and temperature effects on fission-gas release from UO_2, Nuclear Science and Engineering 38 (1969) 143–155.

[7] Rest, J. and Gehl, S. M, The mechanistic prediction of transient fission-gas release from LWR fuel, Nuclear Engineering and Design 56 (1980) 233–256.

[8] I. J. Hastings, A. D. Smith, P. J. Fehrenbach, T. J. Carter, Fission gas release from power-ramped UO_2 fuel, Journal of Nuclear Materials 139 (1986) 531–543.

[9] C. T. Walker, P. Knappik, M. Mogensen, Fission gas release from power-ramped UO_2 fuel, Journal of Nuclear Materials 161 (1988) 10–23.

[10] R. J. White, R. C. Corcoran, P. J. Barnes, A summary of swelling data obtained from the AGR/Halden Ramp Test Programme, Tech. Rep. R&T/NG/EXT/REP/0206/02 (2006).

[11] M. J. F. Notley, J. R. MacEwan, Stepwise release of fission gas from UO_2 fuel, Nuclear Applications 2 (1966) 477.

[12] E. Rothwell, The release of Kr^{85} from irradiated uranium dioxide on post-irradiation annealing, Journal of Nuclear Materials 5 (1962) 241–249.

[13] K. Une, S. Kashibe, Fission gas release during post irradiation annealing of BWR fuels, Journal of Nuclear Science and Technology 27 (1990) 1002–1016.

[14] J. Nakamura, M. Suzuki, H. Uetsuka, Re-irradiation tests of LWR spent fuel at JMTR, in: Enlarged Halden Programme Group Meeting, Loen, Norway, May 24–29, 1999.
[15] E. Sartori, J. Killeen, J. A. Turnbull, International Fuel Performance Experiments (IFPE) database, OECD-NEA, 2010, available at http://www.oecd-nea.org/science/fuel/ifpelst.html.
[16] G. Ducros, Y. Pontillon, P. P. Malgouyres, Synthesis of the VERCORS experimental program: Separate-effect experiments on fission product release, in support of the PHEBUS–FP programme, Annals of Nuclear Energy 61 (2013) 75–87.
[17] W. Hering, The KWU fission gas release model for LWR fuel rods, Journal of Nuclear Materials 114 (1982) 41–49.
[18] Y. H. Koo, B. H. Lee, D. S. Sohn, COSMOS: a computer code to analyze LWR UO_2 and MOX fuel to high burnup, Annals of Nuclear Energy 26 (1999) 47–67.
[19] L. C. Bernard, J. L. Jacoud, P. Vesco, An efficient model for the analysis of fission gas release, Journal of Nuclear Materials 302 (2002) 125–134.
[20] Y. Rashid, R. Dunham, R. Montgomery, Fuel Analysis and Licensing Code: FALCON MOD01, Volume 1: Theoretical and Numerical Bases, Tech. Rep. EPRI 1011307, Electric Power Research Institute (2004).
[21] P. Van Uffelen, A. Schubert, J. van de Laar, C. Györi, Development of a transient fission gas release model for TRANSURANUS, in: Water Reactor Fuel Performance Meeting, Seoul, Korea, October 19–23, 2008.
[22] G. Pastore, D. Pizzocri, J. D. Hales, S. R. Novascone, D. M. Perez, B. W. Spencer, R. L. Williamson, P. Van Uffelen, L. Luzzi, Modelling of transient fission gas behaviour in oxide fuel and application to the BISON code, in: Enlarged Halden Programme Group Meeting, Røros, Norway, September 7–12, 2014.
[23] D. Pizzocri, G. Pastore, T. Barani, E. Bruschi, L. Luzzi, P. Van Uffelen, Modelling of Burst Release in Oxide Fuel and Application to the TRANSURANUS Code, in: 11^{th} International Conference on WWER Fuel Performance, Modelling and Experimental Support, Varna, Bulgaria, September 26–October 3, 2015.
[24] K. Lassmann, The structure of fuel element codes, Nuclear Engineering and Design 57 (1980) 17–39.
[25] Fuel modelling at extended burnup (FUMEX-II), Tech. Rep. IAEA-TECDOC-1687, International Atomic Energy Agency (2012).
[26] Improvement of computer codes used for fuel behaviour simulations (FUMEX-III), Tech. Rep. IAEA-TECDOC-1697, International Atomic Energy Agency (2013).
[27] R. L. Williamson, J. D. Hales, S. R. Novascone, M. R. Tonks, D. R. Gaston, C. J. Permann, D. Andrs, R. C. Martineau, Multidimensional multiphysics simulation of nuclear fuel behavior, Journal of Nuclear Materials 423 (2012) 149–163.
[28] K. Lassmann, TRANSURANUS: a fuel rod analysis code ready for use, Journal of Nuclear Materials 188 (1992) 295–302.
[29] J. D. Hales, R. L. Williamson, S. R. Novascone, G. Pastore, B. W. Spencer, D. S. Stafford, K. A. Gamble, D. M. Perez, R. J. Gardner, W. Liu, BISON theory manual: The equations behind nuclear fuel analysis, Tech. Rep. INL/EXT–13–29930, Rev. 1, Idaho National Laboratory, ID, USA (2014).
[30] G. Pastore, L. P. Swiler, J. D. Hales, S. R. Novascone, D. M. Perez, B. W. Spencer, L. Luzzi, P. Van Uffelen, R. L. Williamson, Uncertainty and sensitivity analysis of fission gas behavior in engineering-scale fuel modeling, Journal of Nuclear Materials 465 (2015) 398–408.
[31] K. Lassmann, A. Schubert, P. Van Uffelen, C. Györi, J. van de Laar, TRANSURANUS Handbook, Copyright ©1975–2014, Institute for Transuranium Elements, Karlsruhe, Germany, 2014.
[32] G. Pastore, L. Luzzi, V. Di Marcello, P. Van Uffelen, Physics-based modelling of fission gas swelling and release in UO_2 applied to integral fuel rod analysis, Nuclear Engineering and Design 256 (2013) 75–86.
[33] M. V. Speight, A calculation on the migration of fission gas in material exhibiting precipitation and re-solution of gas atoms under irradiation, Nuclear Science and Engineering 37 (1969) 180–185.
[34] M. S. Veshchunov, Modelling of grain face bubbles coalescence in irradiated UO_2 fuel, Journal of Nuclear Materials 374 (2008) 44–53.
[35] M. V. Speight, W. Beere, Vacancy potential and void growth on grain boundaries, Metal Science 9 (1975) 190–191.
[36] A. R. Massih, K. Forsberg, Calculation of grain boundary gaseous swelling in UO_2, Journal of Nuclear Materials 377 (2008) 406–408.
[37] C. Baker, J. C. Killeen, Fission gas release during post irradiation annealing of UO_2, in: International Conference on Materials for Nuclear Reactor Core Applications, Bristol, United Kingdom, October 27–29, 1987.
[38] G. J. Small, Fission gas release and bubble development in UO_2 during high temperature transients, in: Proceedings of the Technical Committee Meeting on Water Reactor Fuel Element Computer Modelling in Steady-State, Transient and Accident Conditions, Preston, United Kingdom, September 18–22, 1988.
[39] R. L. Williamson, K. A. Gamble, D. M. Perez, S. R. Novascone, G. Pastore, R. J. Gardner, J. D. Hales, W. Liu, A. Mai, Validating the BISON fuel performance code to integral LWR experiments, Nuclear Engineering and Design 301 (2016) 232–244.
[40] J. A. Turnbull, C. A. Friskney, J. R. Findlay, F. A. Johnson, A. J. Walter, The diffusion coefficients of gaseous and volatile species during the irradiation of uranium dioxide, Journal of Nuclear Materials 107 (1982) 168–184.
[41] K. Lassmann, H. Benk, Numerical algorithms for intragranular fission gas release, Journal of Nuclear Materials 280 (2000) 127–135.
[42] K. Forsberg, A. R. Massih, Fission gas release under time-varying conditions, Journal of Nuclear Materials 127 (1985) 141–145.
[43] P. Hermansonn, A. R. Massih, An effective method for calculation of diffusive flow in spherical grains, Journal of Nuclear Materials 304 (2002) 204–211.
[44] M. I. Mendelson, Average grain size in polycrystalline ceramics, Journal of the American Ceramic Society 52 (1969) 443–446.
[45] J. B. Ainscough, B. W. Oldfield, J. O. Ware, Isothermal grain growth kinetics in sintered UO_2 pellets, Journal of Nuclear Materials 49 (1973) 117–128.
[46] N. Cayet, Investigation of delayed fission gas release, Tech. Rep. HWR 488, OECD Halden Reactor Project (1996).
[47] The Third Risø Fission Gas Project: Bump test AN3 (CB8-2R), Tech. Rep. RISØ-FGP3-AN3, OECD Halden Reactor Project (1990).
[48] M. Mogensen, C. Bagger, C. T. Walker, An experimental study of the distribution of retained xenon in transient-tested UO_2 fuel, Journal of Nuclear Materials 199 (1993) 85–101.
[49] K. Lassmann, C. T. Walker, J. van de Laar, F. Lindström, Modelling the high burnup UO_2 structure in LWR fuel fuels, Journal of Nuclear Materials 226 (1995) 1–8.
[50] J. Spino, D. Baron, M. Coquerelle, A. D. Stalios, High burn-up rim structure: evidences that xenon-depletion, pore formation and grain subdivision start at different local burn-ups, Journal of Nuclear Materials 256 (1998) 189–196.
[51] D. Pizzocri, C. Rabiti, L. Luzzi, T. Barani, P. Van Uffelen, G. Pastore, PolyPole-1: An accurate numerical algorithm for intra-granular fission gas release, Journal of Nuclear Materials 478 (2016) 333–342.